
Article:
Buckley-Johnstone, L.E., Trummer, G., Voltr, P. et al. (4 more authors) (2019) Assessing the impact of small amounts of water and iron oxides on adhesion in the wheel/rail interface using High Pressure Torsion testing. Tribology International, 135. pp. 55-64. ISSN 0301-679X

https://doi.org/10.1016/j.triboint.2019.02.024

Assessing the impact of small amounts of water and iron oxides on adhesion in the wheel/rail interface using High Pressure Torsion testing

L.E. Buckley-Johnstone[1], G. Trummer[2], P. Voltr[3], A. Meierhofer[2], K. Six[2], D.I. Fletcher[1], R. Lewis[1*]

[1]The University of Sheffield, UK
[2]Virtual Vehicle Research Center, Graz, Austria
[3]The University of Pardubice, Czech Republic

Abstract

A new High Pressure Torsion (HPT) set-up has been developed for assessing the effect of third body materials in the wheel/rail interface in a representative and controlled manner. In this study the technique has been used to investigate the effect of small amounts of water and iron oxides mixtures when subjected to different contact pressures. HPT tests showed reduction in adhesion relative to a dry contact when testing with small amounts of water and/or oxides, however sustained low adhesion ($\mu<0.05$) was not produced. To aid interpretation of the results a model has been developed to explore the behavior encountered when testing with water and iron oxide mixtures. The model relates the shear properties of water and oxide mixtures (with increasing solid content) to a predicted adhesion. The model shows a narrow window of water to oxide fraction is required for reduced adhesion, particularly on rough surfaces, and this correlates with the behavior observed.

1 Introduction

Low adhesion has been a consistent problem on railways networks around the world. It can cause a safety problem in braking and delays in traction. With train speeds increasing, and time between trains reducing to get the optimum network utilisation, either can be very costly.

It is well known that leaves cause a large problem, particularly in the Autumn season. Analysis of the incidents occurring in this period resulting from low adhesion events such as Signals Passed at Danger (SPADs) and station overruns [1], has shown that at least 50% do not, however, involve leaves, but arise due to “wet-rail” syndrome, where low adhesion results from a small amount of water present on the rail head. This was confirmed by analysis of the incident time which revealed that most non-leaf incidents occurred in the morning or evening around the dew point where a thin film of water would form on the rail head. There is no information available to indicate exactly what level of moisture is critical. This is probably due to the fact that these conditions are highly transitory and investigations of low adhesion incidents tend to take place well after the environmental conditions have changed.

Previous experimental testing has shown that friction levels reduce when a wet-contact begins to dry out [2][3];. One example is illustrated in Figure 1, where water was applied to a twin disc contact and then stopped and the contact allowed to dry out. It is thought in both cases shown that the small amount of water combined with solid material, such as oxides generated in the contact, was responsible for the drop

in adhesion. In neither case, however, was ultra-low (<0.05) adhesion achieved, that would lead to the train incidents described above.

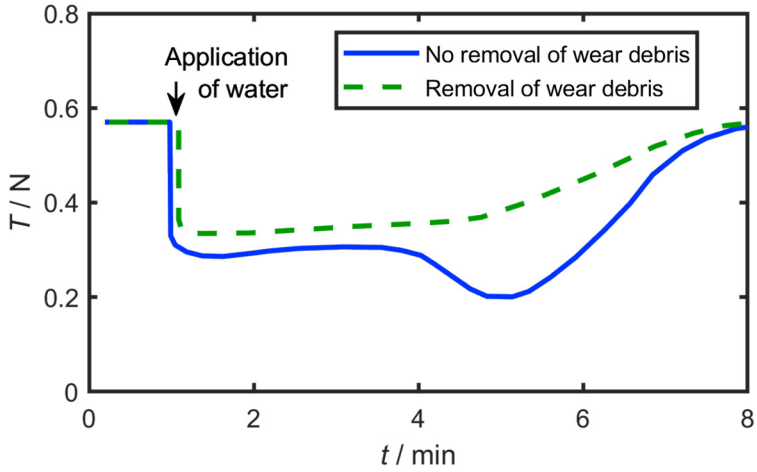

Figure 1: Results from Amsler twin disc experiments [2] showing that wear debris (iron oxides) are necessary to significantly reduce the adhesion T/N (where T and N are the tangential and normal forces, respectively).

There has been other work undertaken to investigate the effects of oxides in a contact. A recent review encapsulates much of this [4]. This focuses mainly on wear effects and environmentally occurring oxides rather than those generated in the contact and illustrates that ultra-low friction values have not been seen in laboratory testing. Other laboratory work has also been carried out investigating water alone [5] and the effect of atmospheric water, as humidity [6], neither of which produced ultra-low levels of adhesion. Researchers have previously investigated water with mini traction machines and have found that water can produce ultra-low levels of adhesion at high velocities on very smooth surfaces [4].

It is clearly very difficult to reproduce the ultra-low adhesion conditions in the laboratory, but it is not evident why. An issue with the testing carried out is that it involves continually cycling over the same specimen surface and is therefore not representative of the field operation. A new test that has emerged recently, based on High Pressure Torsion Testing (HPT), which could help eliminate this problem as it allows a creep curve to be generated in less than one rotation of the contacting specimens [7]. Although the HPT test set-up is not a rolling-sliding contact - which is the case for a wheel/rail contact - the contact is comprised of areas of partial sliding as rotation is increased. The advantage of the HTP setup is the specimens are flat which allows a more accurate application of a third body material, without a rotating body which

The aims of this work were therefore: initially to quantify the levels of water present on a rail head at dew point environmental conditions; to use an HPT test to assess the impact on adhesion of these water levels along with applied and pre-generated oxides; and to develop a physical model on the interface to understand the key parameters involved in the low adhesion mechanism.

HTP testing was undertaken and is described in Section 3, but to plan this main test series it was important to better understand the level of moisture needed to achieve low adhesion conditions. From a review of the literature no information regarding the amount of water formed on the rail surface through water condensing from the

surrounding air could be obtained. There is often anecdotal evidence of low adhesion at the on-set of rain, particularly fine rain or drizzle. A starting point of a suitable estimation of expected water amounts present at low adhesion conditions can be made from using the classification of drizzle rainfall rates. The amount of water present on the surface of the rail through atmospheric water vapour was investigated using controlled testing in an environment chamber. This was then compared to the amounts of water as a consequence of drizzle falling on a flat surface of equivalent area. It thought that the amounts from drizzle would be comparable to those measured at dew point.

2 Water quantification

To give a basis for amounts of water that are expected to form on the rail head at dew point a small scale test was conducted. As these results have been used to inform the HPT tests an overview of the water quantification testing is presented below.

2.1 Apparatus and Methodology

The water quantification test equipment is shown in Figure 2, comprising a rail placed in a one metre cubic environment chamber (Espec ET34) capable of controlling the temperature and relative humidity (RH). Humidity is monitored using a wet bulb and dry bulb thermometers. Dry and wet air is pumped in as necessary to achieve the set RH.

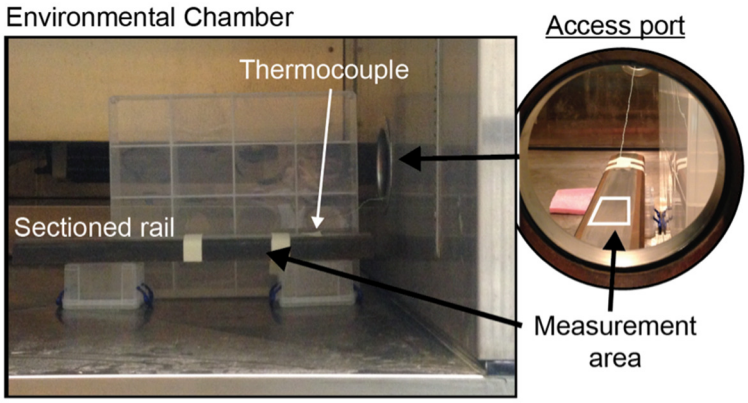

Figure 2: Water quantification test set-up.

A section of rail with a flat top was selected to accurately measure the surface area of interest that was marked out as 100 × 50 mm, across which water condensation was quantified. A digital scale with a measurement accuracy of ±5 µg was used to measure the mass gain of blotting paper after wiping water from this area of the rail head.

Prior to testing the rail head was wiped dry with a clean cloth and samples of the water condensing onto the rail head were taken after 5, 30, 60, 90 and 120 seconds. Each measurement was taken a total of 3 times and an average mass gain was taken. Rail temperature was initially 3ºC prior to the introduction into the chamber, but would rise throughout testing, in some cases rising above the dew point temperature.

2.2 Results

Results have been plotted as volume of water per 100 mm^2 (chosen as an average rail-wheel contact patch size) and are shown in Figure 3. Mass measurements were converted to volumes with an assumed standard density of water (ρ = 1000 kg/m^3).

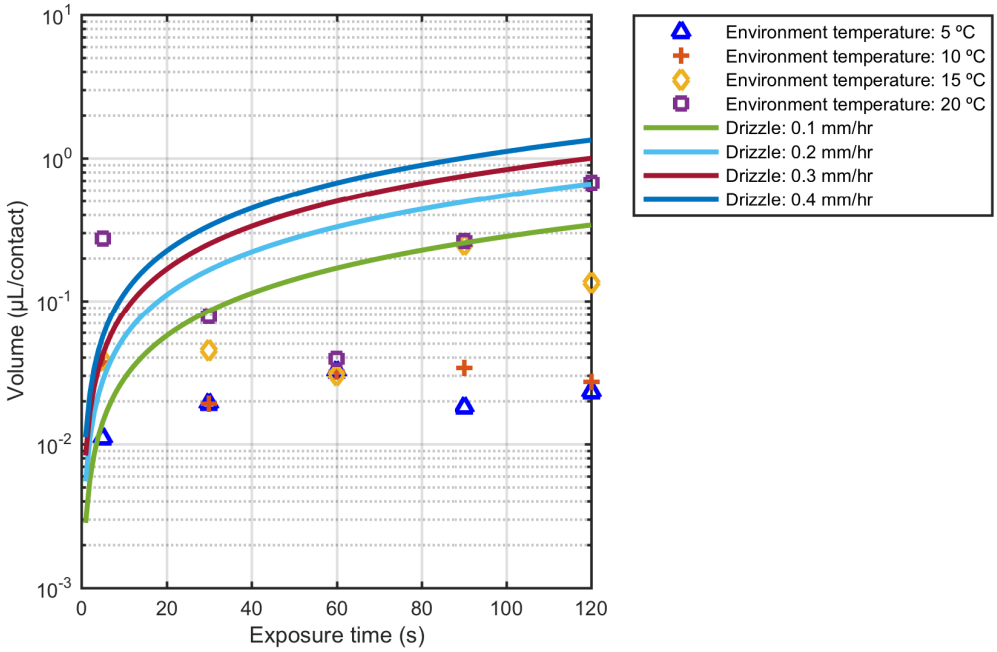

Figure 3: Volume of measured water at set environment temperatures over different exposure lengths. Average drizzle data has been plotted to show range of water amounts.

The experiment had limitations, including uncontrolled rail temperature (rising throughout), poor humidity control and sampling that was not restricted to measuring the water only (i.e., other rail head contaminants could be collected). When considering real-world conditions, the difference between a section of rail in direct sunlight versus a section in the shade may also be significant. However, even with these limitations, the measured amounts fell within the range of average amounts of drizzle. The range of average water volume from these measurements is 0.01 – 0.68 µL per 100 mm^2.

Using these values of water amounts generated environmentally, in conjunction with data on drizzle, water coverage can be defined. Considering equipment limitations the amounts of water that were investigated ranged 0.5 µL / 100 mm^2 to 12 µL / 100 mm^2. The lower value being within the range of volumes measured in the environment chamber, and the upper value representing a surface that has been further wetted - for example this could be from an increased exposure length or a higher rainfall rate.

3 High Pressure Torsion testing

3.1 Apparatus

The HPT rig (shown in Figure 4) is an adapted hydraulic test rig that applies a constant normal load between two specimens whilst rotating one specimen relative to the other at a fixed speed. A tension-compression-torsion load cell measures the normal and torque force whilst a Rotary Variable Differential Transformer (RDVT) measures the rotational speed.

Upon the initiation of the (slow) rotation, there is a period of sharply increasing friction, followed by a gradual transition towards a slightly increasing friction regime. Upon entering steady state sliding the friction levels remains relatively steady with increasing displacement (see Figure 5) and this curve can be converted to a creep curve. Linear displacement is related to the effective radius of the upper specimen, this radius is defined in equation 2. Initial research on this as a test method for assessing wheel/rail contact issues is described by Evans [7]. Although the HTP is not a rolling-sliding contact, as found in the wheel-rail contact, the contact comprises areas of variable sliding across the contact radius. This is akin to that of a rolling sliding contact and is previously described by Evans [7].

Any rail-wheel contaminants of interest can be applied to the specimen surface prior to bringing the surfaces into contact. The effect third body materials have on the torque required to rotate the surfaces against one another can be investigated. The friction effects of the third body layer can then be better understood.

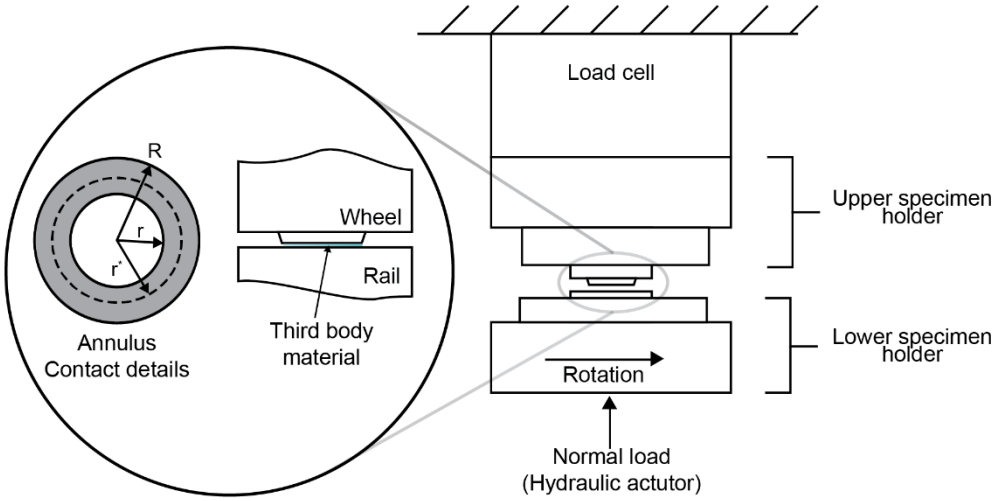

Figure 4: High Pressure Torsion rig schematic diagram showing contact patch area.

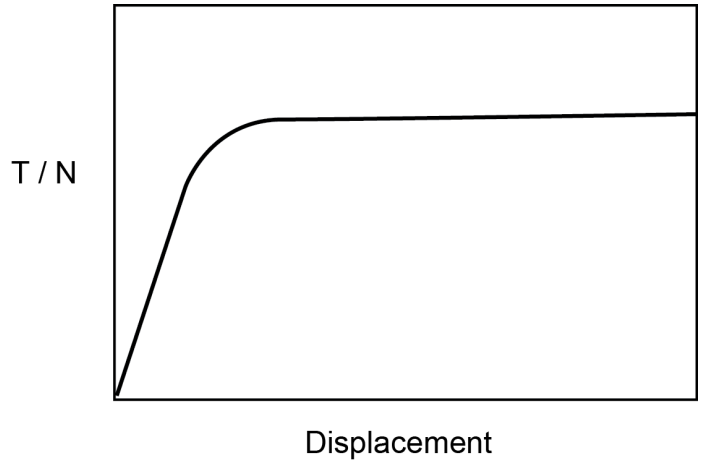

Figure 5: An example of the output of a HPT test.

Wheel and rail specimens were manufactured from R8T wheel steel and 260 grade rail steel respectively. The wheel specimen has an annulus that is in contact with the flat surface of the rail specimen. This creates a contact patch, as seen in Figure 6, with a standard contact area of 167.9 mm^2. The standard initial roughness (R_a) of both specimens is 0.5 µm.

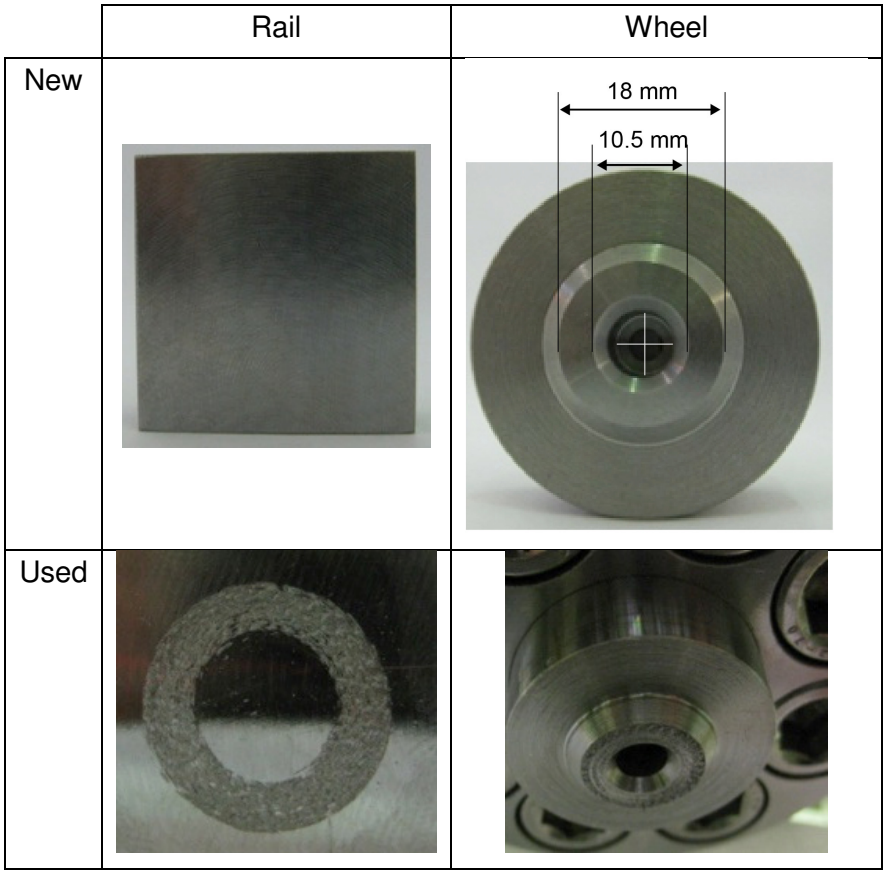

Figure 6: New and used HPT specimens contact surfaces. Clockwise from top left: new rail specimen; new wheel specimen; used wheel specimen (in-situ); used rail specimen.

The normal force is related to the average pressure and the radii of the outer and inner circles by:

$$Pressure = \frac{Force}{Area} = \frac{Applied\ load}{\pi(R^2 - r^2)} \quad (1)$$

3.2 Methodology

The process to generate a displacement curve using the HPT rig was the same for both dry and contaminated tests. Roughness measurements are taken prior to testing to ensure the initial surface roughness of each set of specimens was within specification.

The test procedure followed was:

1. Check contact patch dimension with pressure sensitive film to ensure load is applied evenly across contact patch and accurate dimensions of contact area can be used for control and later analysis.
2. Clean test specimens surfaces with acetone
3. Apply third body material to rail specimen if required
4. Load specimens into contact and apply required normal load.
5. Lower specimen is rotated at a fixed rate through 0.4 mm (according to the effective radius) and the torque is measured.
6. Unload applied torque.
7. Remove normal load and separate specimens.
8. Rotate bottom specimen to new start point and repeat steps 3-6 (and 2 if required).

Figure 7 shows measured values of normal load and torque during steps 4 to 6 from a typical run. Note that the normal load is negative in compression.

In step 8, if there are to be further tests on the same sample, there is rotation to a new start point that ensures that the initial contact points between specimens is not the same for consecutive tests. The minimum rotation between consecutive tests is 10 degrees. It has been previously found that less rotation will generate a curve with a secondary plateau [7].

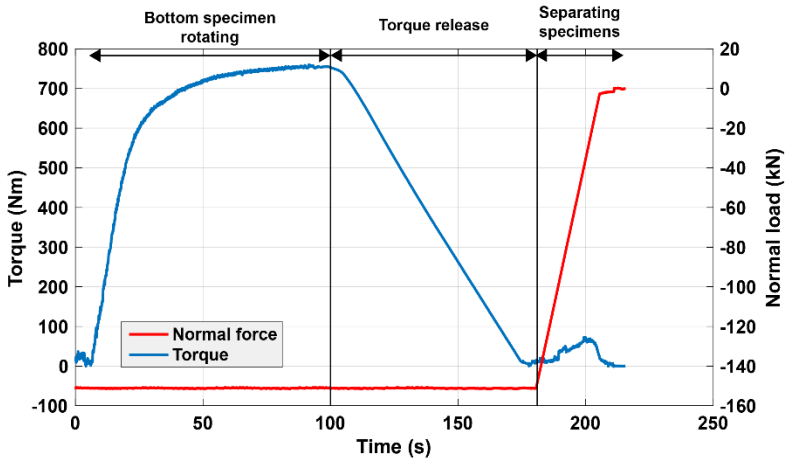

Figure 7: An example of the raw data taken from the HPT test results showing phases 4 through 6.

Following testing the torque data was processed to produce the average shear force at each measured point. It is assumed that the average shear force can be calculated as the measured torque divided by the effective radius:

$$Shear\ force = \frac{measured\ torque}{effective\ radius} = \frac{measured\ torque}{\frac{2}{3}(\frac{R^3-r^3}{R^2-r^2})} \quad (2)$$

This shear force can then be converted to a creep stress in the contact. Again, it is assumed that the creep stress is uniform across the contact:

$$Creep\ stress = \frac{shear\ force}{measured\ contact\ area} \quad (3)$$

For comparison with twin disc tests or data from track the coefficient of adhesion T/N was calculated (shear force divided by normal load) and plots of displacement against friction for each condition are produced.

Displacement is calculated as the length of arc travelled using the effective radius. An angle of 3.2 degrees will produce a 0.4 mm arc at an effective radius of 7.289 mm. The exact angle for a given test varied depending on the measured radii to achieve contact displacement of 0.4 mm.

Measurements of surface roughness were made using a stylus profilometer (Mitutoyo Surftest SJ-400) before and after each set of tests. Roughness measurements required the removal of specimens; consequently these measurements were restricted to measuring the final roughness of a test specimen after they had been subjected several loading cycles.

Measurements of environmental temperature and air humidity of the laboratory were recorded, but were not a controlled variable.

3.3 Test conditions

The investigation variables of interest were:

- Load, surface condition
- Variable amounts of water + iron oxide mixtures (including water alone)

An initial investigation to produce baseline creep curves and assess the effects of repeated use of specimens was completed. The standard test conditions are shown in Table 1.

Table 1: Standard HPT test conditions

Speed (deg/s)	Distance (mm)	Effective radius (mm)	Area (mm^2)	Temperature	Humidity
0.04 – 0.2	0.4	7.289	167.9	Room	Room

The normal pressure range tested was between 200 – 1000 MPa. A pressure of 600 MPa was selected to investigate in contaminated conditions as this represents a typical contact pressure between a wheel tread and a top of rail (Lewis, 2004).

The iron oxides used in this study were hematite (Fe_2O_3) and magnetite (Fe_3O_4), both known to be found in the wheel/rail contact (Lewis et al., 2012). Tests using water and iron oxides mixtures at different mass ratios were performed. Oxide component masses relative to the measured amounts of water present on the rail

head were investigated from 50% to 90% by oxide fraction. The amount of iron oxide is calculated from a fixed water component mass in all cases. In this way the volume of water could be kept constant. All contaminants are applied to the rail specimen immediately prior to testing.

4 Results

The results are presented in Figures 8 – 11. Presented data shows the effects that load, run-in and contaminant (water, iron oxide and water + iron oxide) have on the friction coefficient with increased displacement. Run-in is the initial phase of contact evolution up to a conformal/steady-state contact. During run-in there are large contact condition changes that will override any effect the third body materials may have on the coefficient of friction.

Figure 8 shows the effect of normal load in dry conditions. There is a similar trend evident for all dry curves showing a slight reduction of the peak friction coefficient with increasing normal load. The peak adhesion is above 0.5 for all loads (max(T/N) > 0.5). These measurements were made on a single set of specimens and have been run until a steady curve is present. Running-in the surface significantly increases the roughness and generates the curves measured.

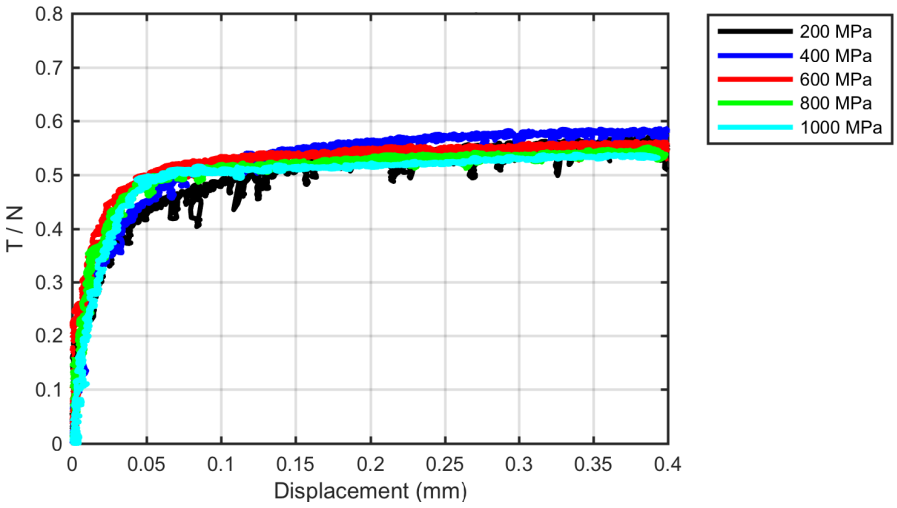

Figure 8: Dry data at different normal pressures showing the coefficient of friction as a function of displacement. Curves shown have been produced using run-in specimens.

The effect of the run-in can be seen in Figure 9, which presents the results from iron oxide tests with zero water. These tests were completed on fresh specimens, and have been plotted against a dry curve that was also performed on unused specimens. The peak coefficient of friction on unused specimens (max(T/N) > 0.7) is reduced upon further working of the surface until to a steady peak value is reached (max(T/N) ≈ 0.55). The results show that oxides alone do not reduce the maximum friction, but have an influence on the curve characteristics. No difference was evident between the two types of oxide.

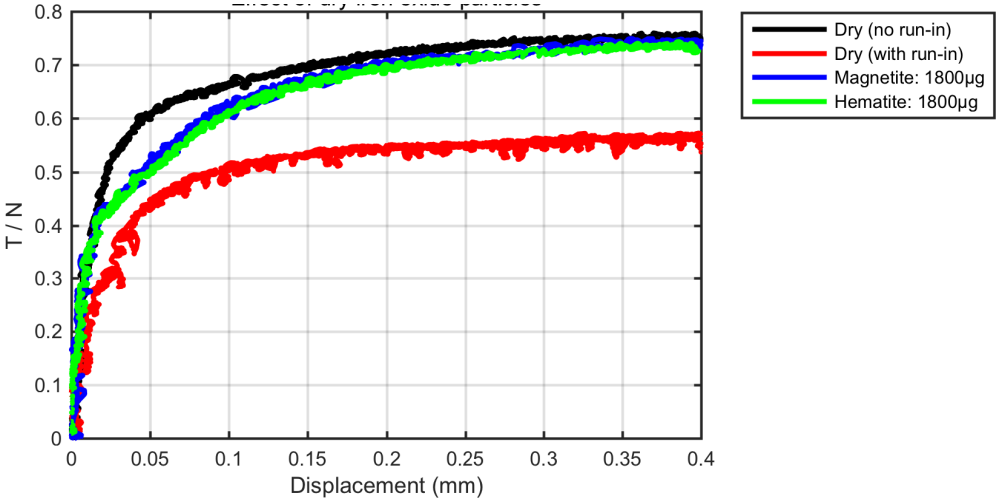

Figure 9: Effect of oxide only as a third body layer when compared to dry conditions with no run-in and dry conditions with a worked surface. Normal pressure: 600 MPa.

Figure 10 shows a clear reduction in adhesion under reduced water conditions. In 'flooded' conditions a large amount of water was placed between the contact. When the amount of water is reduced the adhesion conditions cause stick-slip of the interface to occur. This can be seen as sudden drops on the plots of 10 µL and 20 µL curves. It is not clear if this is a result of dynamic effects in the rig or interface conditions. Further dynamic modelling is under way to investigate this phenomenon.

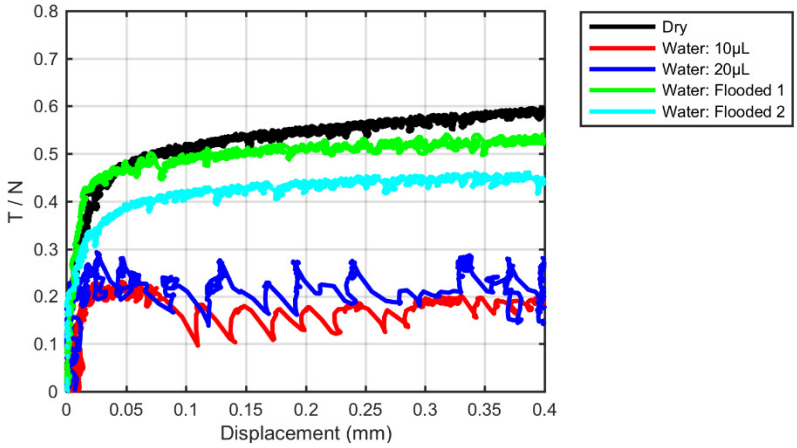

Figure 10: Effect of a range of amounts of water on a HPT test. Dry data has been plotted for comparison. Normal pressure: 600 MPa

Figure 11 shows a sample of the iron oxide + water results. Reduced friction is apparent and the stick-slip behavior occurred again. However, the ultra-low levels of adhesion were not sustained.

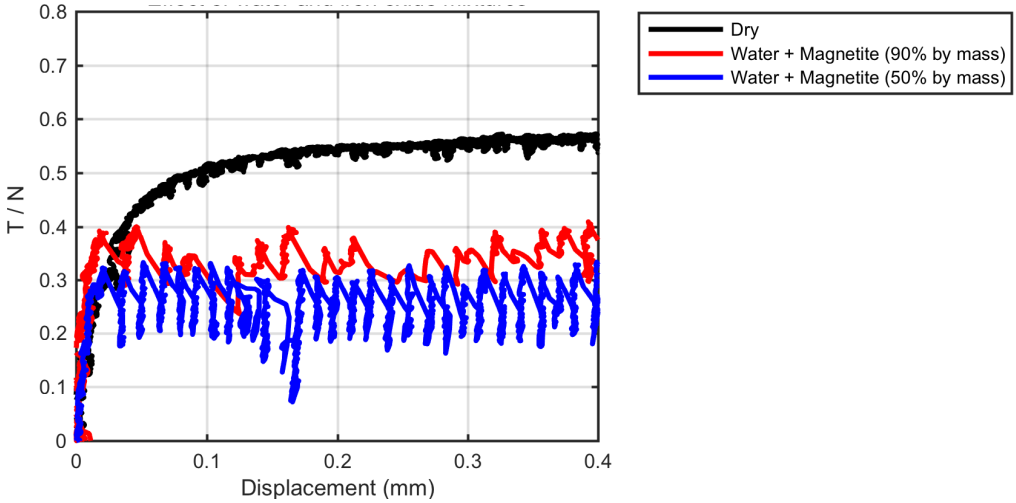

Figure 11: Effect of a range of water + iron oxide (magnetite) on a HPT test. Dry data has been plotted for comparison. Normal pressure: 600 MPa.

Having captured behaviors from the HPT test configuration under conditions relevant to rail-wheel contact an adhesion model was developed to explore how the effect of water and surface oxides may combine to produce the adhesion levels observed.

5 Adhesion Model

5.1 Background and Development

In the HPT tests in this study and, as mentioned above, in twin disc experiments, an adhesion minimum has been observed when a mixture of iron oxide and water is drying up [2]. This has been attributed to the separation of the surfaces by changes of the yield stress and the viscosity of a mixture of iron oxide and water in the contact [10]. Here the possibility to separate rough surfaces as a result of the yield stress of an iron oxide and water mixture in case of quasi-static HPT conditions is explored to try and understand the key conditions leading to low adhesion.

The so-called “adhesion model” is intended to describe the change in adhesion under quasi-static conditions in a qualitative way when a “paste-like” mixture of iron oxide and water is present in the contact. The term “quasi-static conditions” refers to conditions in which the normal load is applied slowly (as in a HPT experiment) and dynamic effects such as the influence of viscosity are neglected. The application of load is much slower compared to typical wheel-rail rolling contact conditions in which loading and unloading of a point on the rail may take place within milliseconds or less.

Key input parameters of the model are the change of shear yield stress of the iron oxide and water mixture with water content, the amount of mixture in the contact and the roughness of the surfaces.

The adhesion model is built around squeeze flow theory and the statistical modelling of rough surfaces. The basic idea is that normal and tangential forces are partly transmitted by solid-solid contact between asperities of the rough surfaces and partly by the mixture of iron oxide and water in the contact. The adhesion f at a macroscopic scale may then be estimated as the sum of the tangential force T_B

transmitted by the asperities and the tangential force transmitted by the iron oxide and water mixture T_C divided by the sum of the normal force carried by the asperities N_B and the normal force N_C carried by the mixture of iron oxide and water.

$$f = \frac{T_B + T_C}{N_B + N_C} \tag{4}$$

Squeeze flow theory is commonly used to investigate the solid and viscous properties of fluids [11]. For such investigations parallel-plate plastometers can be used where material is compressed between two parallel circular plates by a normal force (see Figure 12) [12]. The normal force N_C required to realize a (static) separation h of the plates after infinite time is a function of the plate radius a, and the shear yield stress τ of the material:

$$N_C = \frac{2\pi a^3 \tau}{3h} \tag{5}$$

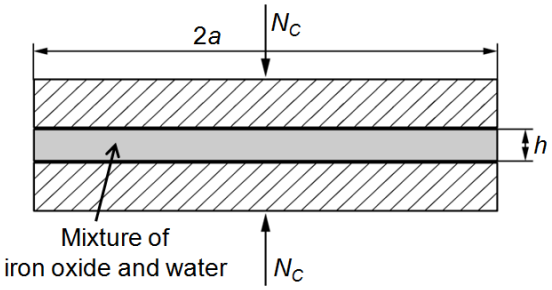

Figure 12: Schematic diagram of a parallel-plate plastometer.

The process of parallel-plate plastometry resembles the compression of a mixture of iron oxide and water in a HPT test as described in Section 3.1.

The relationship of the normal force N_B, the contact area associated with asperity contact A_B and the approach of the surfaces h^* with respect to the mean asperity height can be described by an analytical approximation in the Greenwood and Williamson model if an exponential distribution of asperity heights are assumed [13]. The following height distribution function ϕ has been suggested as an approximation for a Gaussian asperity height distribution when the focus is on large asperity heights [13]:

$$\frac{\phi}{\sigma} = 17e^{-3\frac{z}{\sigma}} \tag{6}$$

z is the height of the asperities measured from the mean asperity height and σ is the standard deviation of asperity heights, which may be substituted by the roughness value R_q. The normal force N_B and the area associated with asperity contact A_B are then given by Polycarpou & Etsion [13]:

$$N_B = 1.933\,\beta E A \sqrt{\frac{\sigma}{R}} e^{-3\frac{h^*}{\sigma}} \tag{7}$$

$$A_B = 5.934\,\beta A e^{-3\frac{h^*}{\sigma}} \tag{8}$$

R is the radius of the asperity summits, E is the composite elastic modulus of the contacting surfaces, A is the nominal contact area and β is a roughness parameter calculated as the product of the areal density of asperities η, the radius of the asperity summits R and the standard deviation of asperity heights σ. The relationship between h^* and the film thickness h (in Eqn. 5) is chosen as:

$$h^* = h - 2R_q \tag{9}$$

Thus the reference height for the film thickness calculation (Eqn. 5) is located two times the standard deviation (of a Gaussian asperity height distribution) below the mean asperity height.

The sum of the normal forces N_C (Eqn. 5) and N_B (Eqn. 7) must equal the given total normal force N, which allows calculating the separation h of the surfaces. The tangential force T_B related to the solid-solid contact is calculated assuming Coulomb friction with the coefficient of friction μ as

$$T_B = \mu\, N_B \tag{10}$$

The tangential force transmitted by the mixture of iron oxide and water is calculated as the shear yield stress τ multiplied by the contact area associated with the mixture of iron oxide and water in the contact $(A - A_B)$.

$$T_C = (A - A_B)\tau \tag{11}$$

In the model the ratio T_c/N_c is limited to an assumed coefficient of friction μ_O associated with dry iron oxide in the contact.

5.2 Results

For the numerical investigation the ring-shaped contact (annulus) of the HPT test is approximated by a circular contact in order to use Eqn. 5 derived from squeeze flow theory. This may be done based on the contact area of a characteristic portion of the annulus. A square of side length of 3.75 mm, which corresponds to the difference of the outer and inner radius of the annulus, is equivalent to a circle with a diameter of 4.23 mm.

Another possibility to calculate an equivalent circular contact is to keep the mean distance of points inside the contact area to the edge of the contact constant. This approach is motivated by the fact that squeeze flow theory is based on the pressure gradient across the contact area. For equivalent contacts this pressure gradient should be similar. For the ring-shaped HPT contact geometry the mean distance of points in the contact area to the edge of the contact is 0.935 mm. A circular contact with a diameter of 5.61 mm has the same mean distance of points inside the contact area to the edge of the contact.

Because it is not clear which method of calculating an equivalent circular contact for the ring-shaped HPT contact geometry is more appropriate it has been decided to use a diameter value in between these two values. Thus a diameter of 5 mm for the equivalent circular contact has been chosen for the subsequent calculations. For this contact the same pressure p_0 as in the HPT test (see Figure 13) is prescribed.

The change of shear yield strength τ with iron oxide fraction in a mixture of iron oxide and water has been taken from literature [10]. Figure 14 shows that a significant shear yield strength of an iron oxide and water mixture can only be observed for iron oxide fractions greater than 95 wt%.

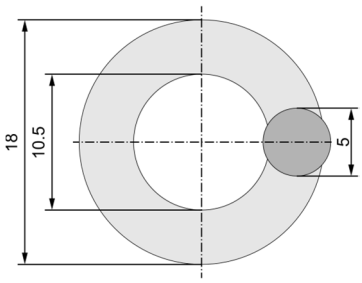

Figure 13: Approximation of the HPT contact geometry (light grey) by a circular contact of $2a$ = 5 mm (dark grey) with identical normal pressure p_0.

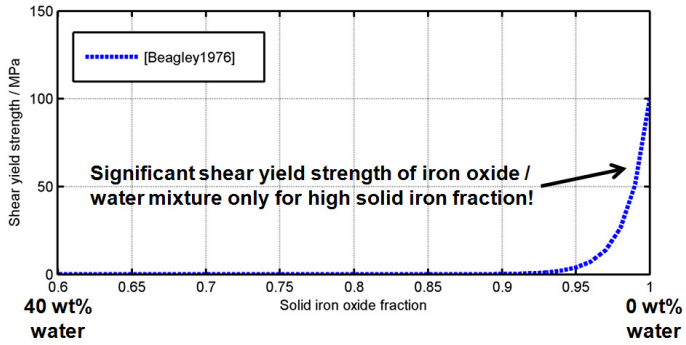

Figure 14: Change of shear yield strength τ of a mixture of iron oxide and water as a function of the solid iron oxide fraction in a mixture of solid iron oxide and water according to (Beagley, 1976).

The standard parameters for the results in Figure 15 and Figure 16 were: normal pressure p_0 = 600 MPa; nominal contact area A = 19.6 mm²; roughness R_q = 10 µm; layer thickness h = 15 µm; elastic modulus E = 210 GPa; roughness parameter β = 0.2; asperity summit radius R = 100 µm; friction coefficients μ = 0.25 and μ_O = 0.35 for wet and dry contacts respectively, unless otherwise stated in the figures. The dry and wet friction coefficients are assumed to be constant for a dry and wet steel-steel contact (i.e. independent of surface roughness).

Depending on the solid iron oxide fraction two different regimes can be distinguished in Figure 15 and Figure 16: iron oxide fractions lower than about 0.90 cause contact conditions where boundary lubricated solid-solid (asperity) contact dominates. The adhesion value equals the friction coefficient for boundary lubrication μ and does not change with solid iron oxide fraction. If the solid iron oxide fraction is larger than about 0.90 the mixture of iron oxide and water is able to separate the surfaces and to carry part of the normal force. Because of the low shear strength of the mixture only limited tangential stresses can be transmitted by the mixture of iron oxide and water. This results in a significant reduction of the adhesion. The increase of adhesion of the (almost) dry oxide/water mixture towards the dry oxide is attributed to the increasing ability of the oxide/water mixture to transmit significant tangential stresses. For dry oxide a coefficient of friction μ_O is assumed which limits the transmittable tangential force. Roughness R_q and the layer thickness h of the iron oxide water mixture in the contact are the two key parameters which govern the adhesion in the model. In case of large roughness values with respect to the thickness of the iron oxide water layers asperity-asperity contact prevails in the model, which results in adhesion values equal to the coefficient of friction for boundary lubrication μ. A reduction in the adhesion can be observed for small

surface roughness values with respect to the thickness of the iron oxide/water layers (see Figures 15 and 16).

The shape of the adhesion as a function of iron oxide fraction (as shown in Figure 15 and Figure 16) is in qualitative agreement with results from twin disc experiments with mixtures of hematite/water [14]. In these experiments coefficients of adhesion $T/N < 0.05$ have been observed – values that are similar to those in Figure 15 and Figure 16. There are however quantitative differences in the location and width of the adhesion minimum.

Experiments on a full-scale test rig showed that in case of little water in the contact and high creepage (to generate wear debris) low adhesion conditions may develop [15]. These results also support the modeling results shown in Figure 15 and Figure 16.

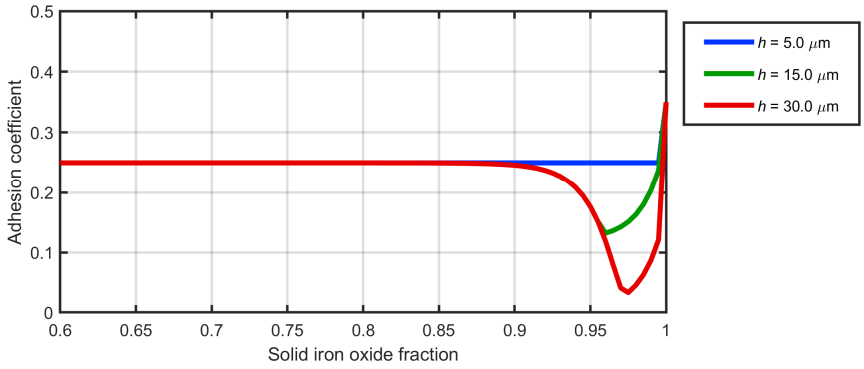

Figure 15: Change of adhesion with solid iron oxide fraction for different values of layer thickness *h*.

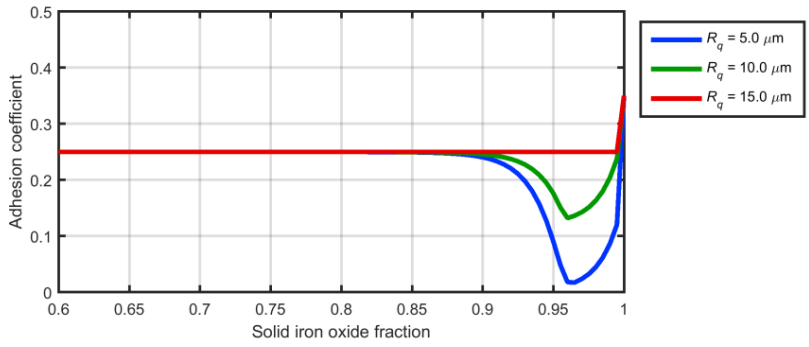

Figure 16: Change of adhesion with solid iron fraction for different roughness values R_q.

Absolute values of the adhesion minima in Figure 15 and Figure 16 need to be treated with caution because the model is only intended to demonstrate the qualitative behaviour of the system. The level of these minima is expected to rise if the iron oxide water mixture is squeezed out of the contact by relative motion of the surface due to creep. This is currently not considered in the model. In addition the influence of the surface roughness on Eqn. 5 has not been investigated and taken into account yet. However, to compensate for the expected increase of the separation h due to the surface roughness, the shear yield strength τ has been used to estimate both the normal force N_C in Eqn. 5 and the tangential force T_c in Eqn. 10.

Despite the simplifications and the limitations of the model, conclusions with regard to the interplay of the amount of water, the amount of iron oxide and the surface roughness with respect to adhesion conditions may be drawn for the design of future

HPT experiments and wheel/rail contact conditions in operation. According to the results a reduction of adhesion due to the presence of iron oxide and low amounts of water in the contact seems feasible in quasi-static conditions as encountered in the HPT experiment, however this reduction of adhesion is limited to a narrow range of conditions.

6 Discussion

HPT tests have been shown to be useful in assessing the effect of third body materials in the wheel/rail interface when testing in a laboratory. Tests under low amounts of water showed a reduction in adhesion over fully flooded interface. Addition of oxide/water mixtures also led to a reduction in friction.

Dry friction levels were as would be expected of steel-on-steel contact and are in line with those previously measured using alternative tribometers [16]. Under dry conditions there is a reduction in the maximum coefficient of friction for a run-in specimen pair. This reduction is evident as a large shift down when compared to a fresh specimen creep curve in similar conditions and will be related to material work hardening and surface roughening.

The run-in of the surfaces in contact also has the effect of increasing the average roughness of surfaces from initial value (R_a = 0.5 µm) in some cases by up to a factor of 20. Where contaminants were included the increase in the roughness was reduced overall, but there were also localised areas of roughening. This roughness increase is a drawback to promoting BL between the specimens.

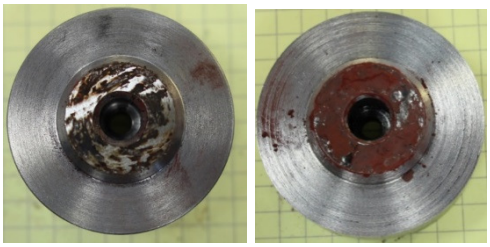

Figure 17: Example of the exposed metal seen post-test.

The developed “adhesion model” is able to relate the flow properties of iron oxide/water mixtures and surface roughness to the adhesion level under quasi-static conditions (slow increase of normal force as in HPT experiments, no relative movement of the surfaces in contact) in order to study the interplay of iron oxide, water and surface roughness in a qualitative way. There is only a small envelope of conditions that leads to low adhesion: a certain amount of oxides depending on the surface roughness, together with the correct low amount of water needs to be present on wheel/rail surfaces. The model results suggest that with a limited amount of iron oxide/water mixture on the surface an increase in surface roughness can effectively prevent the development of low adhesion conditions. The results of the adhesion model with respect to the influence of water are qualitatively in accordance with results from High Pressure Torsion experiments where minimum adhesion was found for low amounts of water under quasi-static conditions and with results from recent Twin Disc experiments [14].

Differences in the absolute values of adhesion might be explained by the difference in contact conditions between HPT testing and a wheel/rail contact. In HPT testing the surface is cleaned prior to testing, whilst a wheel/rail contact will never have a

fully clean and dry contact. The surface stress distribution between a wheel/rail rolling contact (elliptic pressure distribution) cannot be simulated fully by a HPT test (constant pressure distribution). It is these differences in the stress conditions that might contribute to the observed differences in adhesion. However, HPT tests are extremely useful to investigate the behavior of different third body layers, the influence of different surface conditions, as well as the reduction of the initial gradient of the creep curve. (Ultra) low adhesion conditions have not yet been found in HPT testing, however, the absolute value of maximum adhesion under dry conditions is higher in HPT testing than those measured on a tram wheel rig [17].

7 Conclusions

The main outcome of the investigations was that significant reduction of friction (over dry conditions) was observed when applying low amounts of water. This reduction is much higher compared to flooded conditions. Ultra-low friction was not achieved in HPT tests, however. This was a result of the difficulties in applying and distributing third body layers and their inevitable evolution during a test.

An adhesion model was developed to get a better understanding of the interplay between iron oxides/wear debris, water and surface roughness under quasi-static conditions (slow increase of normal force typical for HPT experiments, no relative movement of the surfaces in contact). The model is in accordance with the experience that low adhesion is predominately observed with low amounts of water and explains the difficulties with accurately testing these mixtures (as seen in the HPT test results).

Tribological testing guided the identification of parameters key to the low adhesion mechanisms such as roughness and amount of water. Furthermore, the general characteristic of the adhesion level as a function of the amount of water predicted by the adhesion model was confirmed under rolling contact conditions by the experiments on a full-scale test rig where it has been used to support the specification of these tests [15]. The modeling results have been further supported by results from Twin Disc experiments [14].

Despite the simplifications and the limitations of the model (only quasi-static conditions / slow application of normal force, influence of traction on the film height not considered), conclusions with regard to the interplay of the amount of water, the amount of iron oxide and the surface roughness with respect to adhesion conditions may be drawn for the design of future HPT experiments and wheel/rail contact conditions in operation. According to the results a reduction of adhesion due to the presence of iron oxide and low amounts of water in the contact is feasible in quasi-static conditions, however, this reduction of adhesion is limited to a narrow range of conditions.

8 Acknowledgements

This work was funded by the Rail Safety and Standards Board (RSSB) and Network Rail within the project T1077.

9 References.

[1] White, B.T., Fisk, J., Evans, M.D., Arnall, A.D., Armitage, T., Fletcher, D.I., Lewis, R., Nilsson, R., Olofsson, O., 2016, “A Study into the Effect of the Presence of Moisture at the Wheel/Rail Interface during Dew and Damp Conditions”, *Journal of Rail and Rapid Transit, Proceedings of the IMechE Part F*. Vol 232, pp979-989

[2] Beagley, T.M., Pritchard, C., 1975, “Wheel/Rail Adhesion - The Overriding Influence of Water”, *Wear*, Vol. 35, No. 2, pp299–313.

[3] Lewis, R., Gallardo-Hernandez, E.A., Hilton, T., Armitage, T., 2009, “Effect of Oil and Water Mixtures on Adhesion in the Wheel/Rail Contact”, *Journal of Rail and Rapid Transit, Proceedings of the IMechE Part F*, Vol. 223, pp275-283.

[4] Zhu, Y., 2018, “The influence of iron oxides on wheel-rail contact: A literature review”, *Proceedings of the IMechE, Part F, Journal of Rail and Rapid Transit*. Vol 232, pp734-743

[5] Chen, H., Ban, T., Ishida, M., Nakahara, T., 2008, “Experimental investigation of influential factors on adhesion between wheel and rail under wet conditions”, Wear, Vol. 265, pp1504-1511.

[6] Zhu, Y., Lyu, Y., Olofsson, O., 2015, “Mapping the friction between railway wheels and rails focusing on environmental conditions”, Wear, Vol. 324–325, pp122-128.

[7] Evans, M.D., Lewis, R., Hardwick, C., Meierhofer, A., Six, K., 2015, “High Pressure Torsion testing of the Wheel/Rail Interface”, *Proceedings of CM2015, 10th International Conference on Contact Mechanics and Wear of Rail/Wheel Systems*, Colorado, USA, 30 August-3 September 2015.

[8] Lewis, R. and Olofsson, U., 2004, “Mapping Rail Wear Regimes and Transitions”, *Wear*, Vol. 257, No. 7- 9, pp721-729.

[9] Lewis, R., Dwyer-Joyce, R.S., Lewis, S.R., Hardwick, C., 2012, “Tribology of the Wheel/Rail Contact: The Effect of Third Body Materials”, *International Journal of Railway Technology*, Vol. 1, No. 1, pp167-194.

[10] Beagley, T.M., 1976, “The Rheological Properties of Solid Rail Contaminants and their Effect on Wheel/Rail Adhesion”, *Proceedings of the Institution of Mechanical Engineers*, Vol. 190, pp419-428.

[11] Engmann, J.,. Servais, C. and Burbidge, A.S., 2005, “Squeeze flow theory and applications to rheometry: A review”, *Journal of Non-Newtonian Fluid Mechanics*, Vol. 132, pp1-27.

[12] Covey, G.H. and Stanmore, R.R., 1981, “Use of the Parallel-plate Plastometer for the Characterisation of Viscous Fluids with a Yield Stress”, *Journal of Non-Newtonian Fluid Mechanics*, Vol. 8, pp249-260.

[13] Polycarpou, A.A. and Etsion, I., 1999, “Analytical approximations in modeling contacting rough surfaces”, *Journal of Tribology*, Vol. 121, pp234-239.

[14] White, B., Laity, P., Holland, C., Six, K., Trummer, G. and Lewis, R., 2018, “Iron Oxide and Water Paste Rheology and its Effect on Low Adhesion in the Wheel/Rail Interface”, *submitted to 11th International Conference on Contact Mechanics and Wear of Rail/Wheel Systems (CM2018), Delft, The Netherlands, September 24-27*.

[15]Buckley-Johnstone, L.E., Trummer, G., Voltr, P., Six, K., Lewis, R., 2019, “Full-scale Testing of Low adhesion effects with small amounts of water in the wheel/rail

interface", *submitted to Journal of Rail and Rapid Transit, Proceedings of the IMechE Part F*.

[16] Gallardo-Hernandez, E. A., and Lewis, R., 2008, "Twin Disc Assessment of Wheel/Rail Adhesion",*Wear*, Vol. 265, No. 9–10, pp1309–1316.

[17] Voltr, P. and Lata, M., 2014, "Transient wheel–rail adhesion characteristics under the cleaning effect of sliding", *Vehicle System Dynamics*, 53, 605-618.